tvst

https://doi.org/10.1167/tvst.8.6.30

Article

SRD005825 Acts as a Pharmacologic Chaperone of Opsin and Promotes Survival of Photoreceptors in an Animal Model of Autosomal Dominant Retinitis Pigmentosa

Chulbul M. Ahmed[1], Brian T. Dwyer[2], Alla Romashko[2], Steve Van Adestine[3], Eun-Hee Park[2], Zhen Lou[2], Devin Welty[2], Serene Josiah[2], Anneli Savinainen[2], Bohong Zhang[2], and Alfred S. Lewin[1]

[1] Department of Molecular Genetics and Microbiology, University of Florida, Gainesville, FL, USA
[2] Shire HGT Inc., a member of the Takeda group of companies, Cambridge, MA, USA
[3] Covance Inc., Madison, WI, USA

Correspondence: Alfred S. Lewin, University of Florida, Department of Molecular Genetics and Microbiology, Box 100266, Gainesville, FL 32610-0266, USA. e-mail: lewin@ufl.edu

Received: 25 June 2019
Accepted: 11 October 2019
Published: 12 December 2019

Keywords: retinitis pigmentosa; pharmacologic chaperone; rhodopsin; mouse model; drug therapy

Citation: Ahmed CM, Dwyer BT, Romashko A, Van Adestine S, Park E-H, Lou Z, Welty D, Josiah S, Savinainen A, Zhang B, Lewin AS. SRD005825 acts as a pharmacologic chaperone of opsin and promotes survival of photoreceptors in an animal model of autosomal dominant retinitis pigmentosa. Trans Vis Sci Tech. 2019;8(6):30, https://doi.org/10.1167/tvst.8.6.30

Purpose: Mutations in *RHO*, the gene for a rhodopsin, are a leading cause of autosomal dominant retinitis pigmentosa. The objective of this study was to determine if a synthetic retinal analogue (SRD005825) serves as a pharmacologic chaperone to promote appropriate membrane trafficking of a mutant version of human rhodopsin.

Methods: A tetracycline-inducible cell line was used to produce human wild-type and T17M opsin. A cell-free assay was used to study the impact of SRD005825 on binding of 9-cis-retinal to wild-type opsin. A cell-based assay was used to measure the effect of SRD005825 on the generation of rhodopsin by spectroscopy and Western blot and the transport of rhodopsin to the cell membrane by confocal microscopy. Mice bearing T17M *RHO* were treated with daily oral doses of SRD005825, and retinal degeneration was measured by spectral-domain optical coherence tomography and, at the conclusion of the experiment, by electroretinography and morphometry.

Results: SRD005825 competed with 9-cis-retinal for binding to wild-type opsin but promoted the formation of rhodopsin in HEK293 cells and the trafficking of T17M rhodopsin to the plasma membrane of these cells. T17M transgenic mice exhibited rapid retinal degeneration, but thinning of the outer nuclear layer representative of photoreceptor cell bodies was delayed by treatment with SRD005825. Electroretinography a-wave and b-wave amplitudes were significantly improved by drug treatment.

Conclusions: SRD005825 promoted the reconstitution of mutant rhodopsin and its membrane localization. Because it delayed retinal degeneration in the mouse model, it has potential as a therapeutic for autosomal dominant retinitis pigmentosa.

Translational Relevance: SRD005825 may be useful as a treatment to delay retinal degeneration in retinitis pigmentosa patients with rhodopsin mutations causing misfolding of the protein.

Introduction

Retinitis pigmentosa (RP) leads to progressive deterioration of the retina and to vision loss in 1 in 3500 to 1 in 4000 people in the United States and Europe,[1] making RP the most common form of inherited retinal degeneration. The disease is genetically heterogeneous, with mutations in over 60 genes responsible for nonsyndromic forms of the disease.[2] A total of 30% to 40% of RP cases are inherited in an autosomal dominant pattern, and mutations in the gene for rhodopsin account for about 25% of autosomal dominant RP (adRP).[3]

Rhodopsin, the photosensitive pigment that initi-

ates the visual signaling cascade, is formed when opsin is covalently bound by 11-cis-retinal. Rhodopsin is densely packed in the rod photoreceptor disc membrane, playing an important role in membrane structure as well as function.[4] Over 150 adRP-causing mutations have been identified in *RHO*, the gene for rhodopsin, and these can be classified depending on their biochemical characteristics.[5,6] A large number of mutations fall into class II, based on their propensity to cause misfolding of rhodopsin. Misfolded rhodopsin stimulates the unfolded protein response[7–9] and activation of endoplasmic reticulum (ER)-associated protein degradation.[10] If protein homeostasis cannot be restored, prolonged ER stress leads to the death of rod photoreceptor cells. Although rod photoreceptor death is cell autonomous, the loss of rods ultimately leads to the death of cone photoreceptors and, thus, loss of central vision and the reorganization of the inner retina.[11–13] Thus, if proper folding of rhodopsin can be restored and rod viability maintained, the catastrophic impact of adRP on central vision should be avoided.

The class II rhodopsin mutation T17M leads to a characteristic degeneration of photoreceptors in the inferior retina, and ophthalmoscope observation reveals signs of severe disease in the inferior retina with relative sparing of the superior hemisphere.[14] Much of what we know about the biochemical impact of this mutation comes from the study of animal models of adRP. In transgenic frogs expressing human rhodopsin, replacement of threonine by methionine at position 17 eliminates the N-linked glycosylation at asparagine 15, leaving only one N-linked glycosylation at asparagine 2.[15] Frogs expressing T17M rhodopsin showed normal localization of rhodopsin to outer segments but increased sensitivity to light-induced retinal degeneration.[16] This light-induced degeneration was eliminated by preventing the binding of 11-cis-retinal by mutation of its binding site or by vitamin A deprivation.

A mouse model of T17M rhodopsin was generated by pronuclear injection of a 17-kb segment of human DNA containing the rhodopsin gene (*RHO*).[17] These mice exhibited complete retinal degeneration by 8 months, but the rate of electroretinography (ERG) decline and of outer and inner segment shortening was reduced by dietary supplementation with vitamin A. These mice are extremely sensitive to light-induced retinal damage, with rod photoreceptor death peaking at 1 day postillumination with bright (15,000 lux) light.[18,19] Even when mice are housed in dim light, the expression of human T17M rhodopsin activates the unfolded protein response, although some rhodopsin traffics to the rod outer segment.[20] At postnatal day 30, vacuoles appear within the outer segments of T17M *RHO* mice, suggesting compromised vesicular traffic.[21] Rod cells die by apoptosis associated with activation of Caspase-7.[22] Abnormal localization of T17M rhodopsin has also been documented in cell lines,[23] and activation of the ATF6 pathway, a component of the unfolded protein response, reduced the accumulation of misfolded rhodopsin.[24]

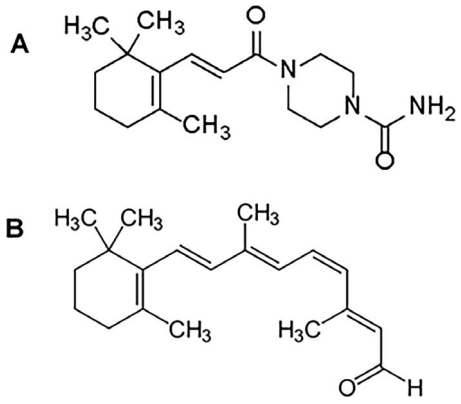

Figure 1. Molecular structure of SRD005825 (A) and 11-cis-retinal (B). Unlike retinal, SRD005825 cannot be converted to retinoic acid, a powerful morphogen.

An attractive approach for the treatment of diseases associated with protein misfolding is the delivery of pharmacologic chaperones, small molecules that shift the folding equilibrium in favor of the native conformation.[25,26] In cell culture, 11-cis-retinal and 9-cis-retinal promote the trafficking of P23H rhodopsin to the cell membrane.[27] Cell-based assays combined with structural analysis has allowed high-throughput screening of potential chaperones to promote rhodopsin folding.[28] These studies confirm the original finding of Li and colleagues[17] that 11-cis retinal promotes the membrane transport of T17M rhodopsin. 9-cis-retinal is an attractive candidate for therapy because it is more stable than 11-cis-retinal,[29] but its metabolic product retinoic acid controls the expression of many genes, making it a potential teratogen.

SRD005825, also known as SHP630 (Fig. 1), is a compound developed for the treatment of adRP. It is an analogue of 9-cis-retinal but cannot serve as a precursor to retinoic acid, and it does not bind covalently to opsin. Relevant to the experiments presented below, it does not have measurable absorbance in the visible spectrum. SHP630 was originally developed by BIKAM Pharmaceuticals

(Cambridge, MA) among a series of small-molecule chaperones for human opsin. Their experiments suggested that the compound induces normal rhodopsin conformation. SHP630 was tested in a transgenic mouse model of human adRP and progressed through a several safety and toxicology studies. BIKAM Pharmaceuticals was acquired by Shire Pharmaceuticals (Cambridge, MA) to continue the development of this compound, now called SRD005825. Earlier work at Shire studied that stability of SRD005825 in hepatic microsomes and its metabolism by cytochrome P450 enzymes.[30,31] In these experiments, we tested the ability of SRD005825 to serve as a pharmacologic chaperone for rhodopsin in a cell-free assay, in cell-based assays using T17M *RHO*, and in the T17M transgenic mouse model of adRP. We found that this compound competed for 9-cis-retinal binding by purified rhodopsin, and in transfected cells it promoted the trafficking of T17M rhodopsin to the cell membrane. In the mouse model of adRP, the orally administered drug was well tolerated and led to significant preservation of retinal structure and function.

Materials and Methods

Cell Lines

Tetracycline-inducible human wild-type and T17M mutant opsin cell lines were developed using the Invitrogen (Waltham, MA) T-Rex system. The growth media was Dulbecco's modified Eagle's medium containing high glucose (Invitrogen) and 5 μg/mL blasticidin at 37°C with 5.0% CO_2. Codon-optimized wild-type and T17M mutant opsin were cloned in the pcDNA4/TO vector (K1020-01; Invitrogen). T-Rex-293 cells passaged under blasticidin selection were transfected by Lipofectamine 2000 followed by Zeocin selection (100 μg/mL). Surviving colonies were screened by quantitative polymerase chain reaction for opsin expression normalized to beta actin expression. Colonies were evaluated for before and after tetracycline-induction by Western blot using the monoclonal antibody 1D4 (ThermoFisher, Waltham, MA). Clones were picked based on the absence of expression before induction, for low, medium, and high levels of opsin after induction, and for good cell viability levels upon passaging.

Purification of Opsin

After 48 hours of induction, wild-type opsin-producing cells were washed with phosphate-buffered saline (PBS) (10 mM sodium phosphate and 130 mM NaCl [pH 7.2]) and lysed in PBSD1 (PBS containing 1.25% n-dodecyl-β-D-maltoside) and complete ethylenediaminetetraacetic acid (EDTA)-free protease inhibitor cocktail tablets (Roche, Basel, Basel Stadt, Switzerland) for 1 hour on ice. The lysate was centrifuged at 40,000 × *g* for 45 minutes, and the supernatant was added to PureCube1D4-coupled Sepharose 4B beads (Cube Biotech, Wayne, PA). A total of 1 mL of settled beads per 50 mL of clarified lysate was incubated for 1 hour at 4°C on a nutator. The beads were transferred to a BioRad (Hercules, CA) (2.5 × 10 cm) column, washed with PBSD1 buffer, followed by PBSD2 buffer (PBS containing 0.125% n-dodecyl-βD-maltoside), and opsin was eluted with a competing peptide corresponding to the last 9 amino acids (TETSQVAPA) of rhodopsin in PBSD2. The purified opsin was dispensed in 0.25- to 0.5-mL aliquots and stored at −80°C for long-term storage.

Competition Assay

The experiment was performed in the darkroom under dim red light. Purified wild-type opsin was thawed at room temperature and diluted to 0.12 mg/mL (3.0 μM) with PBSD2 buffer and incubated with 0, 20, 40, or 80 μM SRD005825 for 5 minutes, followed by the addition of 2.0 μM 9-cis-retinal. Absorbance at 490 and 600 nm was measured every 2 minutes for 60 minutes by using a SpectraMax PLu384 microplate reader (Molecular Devices, San Jose, CA) to monitor formation of rhodopsin. To eliminate background noise, the absorbance value at 600 nm was subtracted from absorbance value at 490 nm. The initial rate of reaction was determined using a negative logarithm of the fraction of maximum rhodopsin formation ($\mathrm{Log}[A_{max}-A]/A_{max}$, where A is adjusted absorbance at 490 nm). The resulting slope of the curve was the initial rate of reaction.[32,33] Half maximal inhibitory concentration (IC_{50}) values were calculated using GraphPad Prism (GraphPad, San Diego, CA), with logarithms of inhibitor concentrations on the x-axis and the initial rate of reaction on the y-axis. A nonlinear regression was used for curve fitting (log dose versus response variable slope stimulation).

9-cis-Retinal Binding to Opsin

All steps were performed in the darkroom under dim red light. A 50 mM stock of 9-cis-retinal in ethanol was prepared by reconstitution of vial of 25

mg of 9-cis-retinal in 1.75 mL of ethanol. It was further diluted with ethanol for binding kinetics study. 9-cis-retinal binding studies utilizing 0.12 mg/mL (3.0 μM) wild-type opsin was mixed with 1, 2, 5, 10, or 20 μM 9-cis-retinal and scanned every 2 minutes for 60 minutes at 490 nm until no more increase in rhodopsin absorbance was detected. The initial rate of reaction was determined as stated above. The kinetics of 9-cis-retinal binding to opsin was described by first-order kinetics ($A = A_0*[1\text{-}e^{-kt}]$). K_M values were determined using SigmaPlot software (Systat, San Jose, CA). Data were analyzed by regression wizard program utilizing ligation binding with one site saturation equation for data fitting, where abscissa was concentration of 9-cis-retinal and the ordinate was initial rate of reaction.

Rhodopsin Regeneration (Rho-gen) Assay

T17M mutant opsin-expressing cells were grown to 80% confluency in 10-cm circular dishes. They were induced (1.0 μg/mL tetracycline) for 2 days in the presence of 0, 0.5, 1.0, 5.0, 10.0, 20.0, 40.0, and 80.0 μM SRD005825. The induction and SRD005825 media were refreshed after the first day of induction. After 2 days of treatment, the cells were washed with cold Dulbecco's PBS (DPBS) (Invitrogen, Waltham, MA). After this, all steps were performed in a dark room under dim red light. The cells were resuspended in 1.0 mL of cold DPBS with 20.0 μM of 9-cis-retinal and nutated for 1.0 hour at room temperature. Following incubation, cells were centrifuged at 1000 rpm and the supernatant was removed. Cells were washed two times with 1.0 mL of cold DPBS. Cells membranes were solubilized with a 1.0% n-dodecyl-βD-maltoside and protease inhibitor cocktail (without EDTA) in cold DPBS for 1 hour at 4°C on a nutator. The solubilized material was centrifuged at 40,000 × g for 10 minutes. The supernatant was added to 1D4 affinity resin pre-equilibrated in DPBS (75-μL bead volume) and nutated for 1 hour at 4°C in a 1.5-mL microtest tube. After the incubation, 1D4 beads were separated by centrifugation and washed three times with 0.1% DM in cold PBS. The 1D4 resin was then washed two times with 0.1% n-dodecyl-βD-maltoside in 10 mM sodium phosphate buffer (pH 6.00). After the last wash, 140 μL of 0.1% n-dodecyl-βD-maltoside in 10 mM phosphate (pH 6.00) and 100 μM 1D4 competing peptide (TETSQVAPA) were added to the resin. The beads were then incubated for 1 hour at 4°C on a nutator. The resin was then pelleted and the tubes held on ice. The eluted protein was analyzed on a Spectra Max Plus spectrophotometer (Molecular Devices) from 250 to 650 nm with increments of 10 nm.[32,34,35]

Sodium Dodecyl Sulfate–Polyacrylamide Gel Electrophoresis (SDS-PAGE) and Immunoblotting

Samples were loaded on 4% to 12% Bis-Tris SDS-polyacrylamide gels and stained with Instant Blue (Sigma-Aldrich, St. Louis, MO). For immunoblotting, the gels were transferred to nitrocellulose membranes using the iBlot system (ThermoFisher, Waltham, MA). Immunoblotting was performed using the iBind system (ThermoFisher). 1D4 antibody in 4% paraformaldehyde in PBS (1:10,000) was used for the primary antibody, and IRDye800TM-conjugated affinity purified goat anti-mouse immunoglobulin G (Licor, Lincoln, NE), diluted 1:10,000, was used for the secondary antibody. The membrane was then washed with iBind Solution and scanned using an Odyssey Infrared imager (Licor, Lincoln, NE).[34,36] Fluorescence intensity was measured using Photoshop CC. A one-way analysis of variance (ANOVA) with Tukey's multiple comparison test was used to establish statistical significance, with $P < 0.05$ considered significant.

PNGaseF Treatment

Some samples prepared for the Rho-gen assay were heat denatured at 100°C for 10 minutes in 0.5% SDS and 40 mM dithiothreitol (this step was omitted for samples that were not treated with glycosidase). After denaturing, 2 μL GlycoBuffer 2 (New England BioLabs, Ipswich, MA), 2 μL 10% NP40, 5 μL H2O, and 1 μL PNGase F (500 units) were added to half of the samples, which were then incubated for 1 hour at 37°C. Reactions were stopped by addition of SDS gel loading dye, and 4 μl of each sample was loaded on a 4% to 12% Bis/Tris gel. Samples were transferred to nitrocellulose and incubated with the 1D4 antibody as described above.

Confocal Microscopy of Membrane-Associated Opsin

Wildtype and T17M mutant opsin-expressing cells cultured as described above were induced with tetracycline in the presence of increasing concentrations of SRD005825, and 24 hours later SRD005825 was reapplied. One day later, cells were fixed in 4% paraformaldehyde in PBS and analyzed by confocal microscopy. Staining with 1D4 monoclonal antibody was used to detect rhodopsin. The plasma membrane

Table 1. PCR Primers for Genotyping

Gene Amplified	Sequence	Annealing Temperature
T17M forward	GAG TGC ACC CTC CTT AGG CA	55°C
T17M reverse	TCC TGA CTG GAG GAC CCT AC	
mRHO forward	GAT TAG CGT TAG TAT GAT ATC TCG	52°C
mRHO reverse	AAG AGA CTC AAG TAA GCT GCA	
rd8 forward 1	GTGAAGACAGCTACAGTTCTGATC	65°C
rd8 forward 2	GCCCCTGTTTGCATGGAGGAAACTTGGAAGACAGCTA	
rd8 reverse	CAGTTCTTCTGGCCCCATTTGCACACTGATGAC	
rd1 sense	CAT CCC ACC TGA GCT CAC AGA AAG	55°C
rd1 antisense	GCC TAC AAC AGA GGA GCT TCT AGC	
RPE65 sense	CAC TGT GGT CTC TGC TAT CTT C	55°C
RPE65 antisense	GGT GCA GTT CCA CTT CAG TT	

was marked by fluorescently tagged wheat germ agglutinin (WGA). Images from 10 replicate wells per treatment were acquired using the Thermo CX7 HCS instrumentation (ThermoFisher) with a 40× objective. Automated quantitative analysis of relative opsin intensity was determined via colocalization analysis of opsin with the membrane fraction of WGA-Alexa Fluor 488 on the analysis suite of the CX7 HCS platform. High-resolution images were taken with a 100× objective on an Echo Revolve microscope (Echo, San Diego, CA). Fluorescence intensity of membrane-bound opsin in each chaperone treated sample was measured and the value compared to the value of treatment with dimethyl sulfoxide (DMSO).

Mouse Strains

All studies were done with prior approval of the University of Florida Institutional Animal Care and Use Committee and in adherence with the ARVO Statement for the Use of Animals in Ophthalmic and Vision Research. T17M *RHO*(+)::*Rho* (+) mice were generated by mating of T17M heterozygous transgenic mice to C57Bl/6BomTac mice. Mice were housed in a dimly lit housing room (50–100 lux) in 12-hour light dark cycle. Genotyping of transgenic mice was performed by PCR of tail biopsy specimens by using the primers listed in Table 1. Conditions of PCR were as follows: 94°C, 2 minutes; 94°C, 45 seconds; annealing (Table 1 for temperatures), 45 seconds; elongation, 72°C, 45 seconds × 30 cycles; and 72°C, 5 minutes. To detect the rd1 mutation, the product was digested with Dde I at 37°C for 30 minutes before running it on a 2% agarose gel. The presence of an undigested 300-bp band suggested the presence of the desired (wild type) genotype. For RPE65, the PCR product was digested with Mwo I at 60°C for 30 minutes before loading on a 2% gel. The presence of a single 700-bp fragment suggested the presence of a RPE65 Met450 sequence typical of C57BL/6 mice. For rd8 genotyping, three primers were used and products were separated on a 4% agarose gel.[37] The wild-type fragment ran at 220 bp, with the rd8 allele migrating at 244 bp.

SRD005825 Dosing

Solutions of the test reagent were made in 0.5% carboxymethylcellulose and 0.1% Tween 80 in water. Stocks of 12 mg/mL (for males) and 24 mg/mL (for females) were prepared by the addition of an appropriate amount of SRD005825 to the solvent and incubation in a sonicating water bath at room temperature for 30 minutes. SRD005825 and vehicle control were given by oral gavage, once every day at 10 AM plus or minus 1 hour. Dosing started at 14 days of age and continued up for 7 weeks (9 weeks of age). SD-OCT was performed 3, 5, and 7 weeks after dosing started. Scotopic and photopic ERG recordings were done 2 hours before the termination of the study and eyes were immediately harvested for histology. At least 2 hours lapsed after the final dose, before ERG recordings were made.

SD-OCT Imaging

High-resolution SD-OCT images were obtained by using Envisu SD-OCT ophthalmic imaging system (Leica Microsystems, Buffalo Grove, IL) as described by Biswal et al.[38] The mice were sedated with ketamine and xylazine as indicated above and placed on a platform. One drop of methylcellulose (2.5%) was placed on each eye prior to analysis. The light emitter and receiving unit (head) was then positioned to make gentle contact with the mouse eye. The outer

nuclear layer (ONL) was measured at four different locations (temporal, nasal, superior, and inferior) at a 0.35-mm distance from the optic nerve head. Following this procedure, antibiotic ointment was applied to prevent dehydration of the cornea and infection. This procedure was performed at baseline (predosing) and following the last dose (day 42).

ERG

To record dark-adapted (scotopic) ERG, mice were placed in the dark for at least 12 hours. The animals were dark adapted overnight. Then, mice were sedated with a mixture of ketamine/xylazine (40–90 mg/kg ketamine and 5–10 mg/kg xylazine). Phenylephrine (2.5%) and atropine sulfate (1%) were dropped into the eye to induce mydriasis. Proparacaine (0.5%) was used as topical anesthetic. Upon completion of mydriasis, one drop of lubricant eye drop (CVS Pharmacy, Gainesville, FL) was dropped onto the corneas to serve as contact solution for the corneal contact lens to measure ERG and to prevent drying of eyes. ERGs were recorded on both eyes simultaneously. Contact electrodes were placed on the cornea. A reference electrode was placed subcutaneously on the head and a ground electrode in the hind leg. Ten flashes each at −20 dB, −10 dB, and 0 dB were directed toward the eyes for scotopic ERG, and the responses were recorded using an LKC apparatus. Bleaching was carried out for 2 minutes, and 10 flashes each at −3 dB, 3 dB, 6 dB, and 10 dB were directed toward the eyes and photopic responses were recorded.

Histology

For histology, eyes were harvested by trimming gently with forceps scissors across the eyeball, and eyes were removed by cutting the optic nerve. Eyes were stored overnight at −4°C in fixative (O-Fix; Leica, Nussloch, Baden-Württemberg Germany), followed by washing and storage in PBS. Fixed tissue was embedded in paraffin, sectioned and stained with hematoxylin/eosin. Quantification was made by measuring the ONL thickness at 3 positions at either side of the optic nerve head. The six measurements were averaged for each eye and the two eyes were averaged for each mouse.

Results

Competition Assay With Wild-Type Opsin

Human opsin was purified from T-Rex-293 cells as described in the Materials and Methods, and a cell-free binding assay with 9-cis-retinal was established so that opsin was saturated at a concentration of 5 μM 9-cis-retinal and that the K_M based on the initial rate of binding varied between 8.09 and 14.6 μM (Supplementary Fig. S1). A competition assay was then performed using 2.0 μM 9-cis-retinal and increasing concentrations of SRD005825. The initial rate of binding of 9-cis-retinal, as measured by A490, was reduced by increasing concentrations of SRD005825 (Figs. 2A, 2B). In three separate experiments, the estimated IC_{50} ranged from 17.8 μM to 28.6 μM (Fig. 2C), although complete competition of 9-cis-retinal binding was not attained due to the irreversible binding of 9-cis-retinal to opsin. We conclude that SRD005825 competes with 9-cis-retinal for binding to opsin.

SRD005825 Promotes Membrane Translocation of T17M Opsin

In cultured cells, T17M opsin accumulates in the ER, but the addition of 11-cis-retinal to the medium increases translocation of rhodopsin to the plasma membrane.[17,39] To test whether SRD005825 increased transport of T17M opsin to the plasma membrane of cells, wild-type and T17M opsin-expressing cells were incubated in the presence of SRD005825, and we measured the level of translocation to the plasma membrane using confocal microscopy (Fig. 3). A substantial fraction of T17M opsin was associated with the ER, as reported by Jiang and colleagues,[23] but the addition of the pharmacologic chaperone promoted an association with the plasma membrane (Fig. 3B). Cells expressing wild-type opsin, in contrast, showed a substantial fraction of opsin associated with the plasma membrane, and the addition of SRD005825 did not increase the association with the plasma membrane (Fig. 3A). When normalized to the DMSO control, we observed a dose-dependent increase in association of T17M opsin with the plasma membrane following treatment with SRD005825 (Fig. 3D) but not for wild-type opsin (Fig. 3C).

SRD005825 Stimulates Regeneration of Rhodopsin

To determine if SRD005825 serves as a pharmacologic chaperone for T17M opsin, we performed a functional assay using T-Rex-293 cells expressing T17M opsin to demonstrate its binding with 9-cis-retinal. We followed the method of Noorwez and colleagues[27,34] who demonstrated that retinal ana-

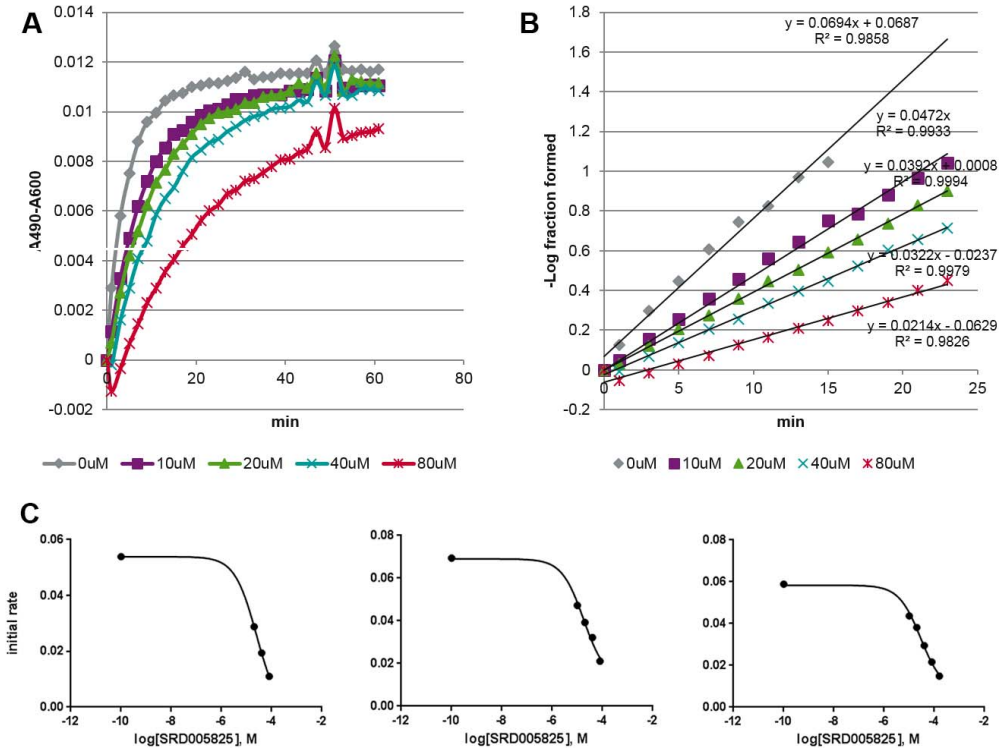

Figure 2. SRD005825 inhibits binding of 9-cis-retinal by wild-type opsin. (A) Competition assay: purified human wild-type opsin was diluted to 0.12 mg/mL (3.0 μM) and incubated with 0, 20, 40, or 80 μM SRD005825 for 5 minutes followed by the addition of 2.0 μM 9-cis-retinal. Absorbance at 490 and 600 nm was measured every 2 minutes for 60 minutes to monitor the formation of rhodopsin. To eliminate background noise, the absorbance value at 600 nm was subtracted from the absorbance value at 490 nm. (B) Initial rates of binding: the initial rate of reaction was determined using a negative logarithm of the fraction of maximum rhodopsin formation ($Log[A_{max}-A]/A_{max}$, where A is adjusted absorbance at 490 nm).[33,34] (C) Results of three separate competition assays. IC_{50} values are estimated because complete competition was not achieved.

logues facilitated the generation of wild-type and P23H rhodopsin in cultured cells expressing these forms of opsin. T17M opsin expression was induced by the addition of tetracycline, and the cells were treated with increasing concentrations of SRD005825 for 48 hours. After the treatment, cells were incubated with 9-cis-retinal to allow binding with T17M opsin to form T17M rhodopsin. The generation of T17M rhodopsin was observed in absorbance spectrum analysis where the rhodopsin peak at 480 nm increased with increasing the concentration of SRD005825 (Fig. 4A). The optical density (OD) 480 nm plotted against concentration of SRD005825 demonstrated a dose-dependent response (Fig. 4B). The same samples containing T17M rhodopsin used for absorbance spectrum analysis were analyzed by Western blot, using the 1D4 antibody that binds to the C-terminus of opsin.[40] An increasing amount of monomeric T17M was observed as the concentration of SRD005825 increased (Fig. 4C). Because this band, as well as the slower migrating species, were replaced by more rapidly than migrating bands following treatment with PNGaseF (Supplementary Fig. S2), they may represent glycosylated forms of rhodopsin. The relative quantity of T17M rhodopsin represented by the mean intensity of the band on Western blot were plotted against the concentration of SRD005825 (Fig. 4D) and demonstrated a dose-dependent response similar to the OD 480-nm measurement (Fig. 4B). The Rho-gen assay was repeated three times, and the plots in Figures 4B and 4D were generated using OD 480-nm values and mean green color intensity from the three independent experiments (Supplementary Table S1). We could not calculate an half maximal effective concentration (EC_{50}) value because SRD005825 was toxic to cells at 80 μM and above. Nevertheless, it appears that SRD005825 increased the amount of T17M opsin that could combine with 9-cis-retinal and be extracted from cell membranes. This chaperone activity was dependent on the dose of the compound.

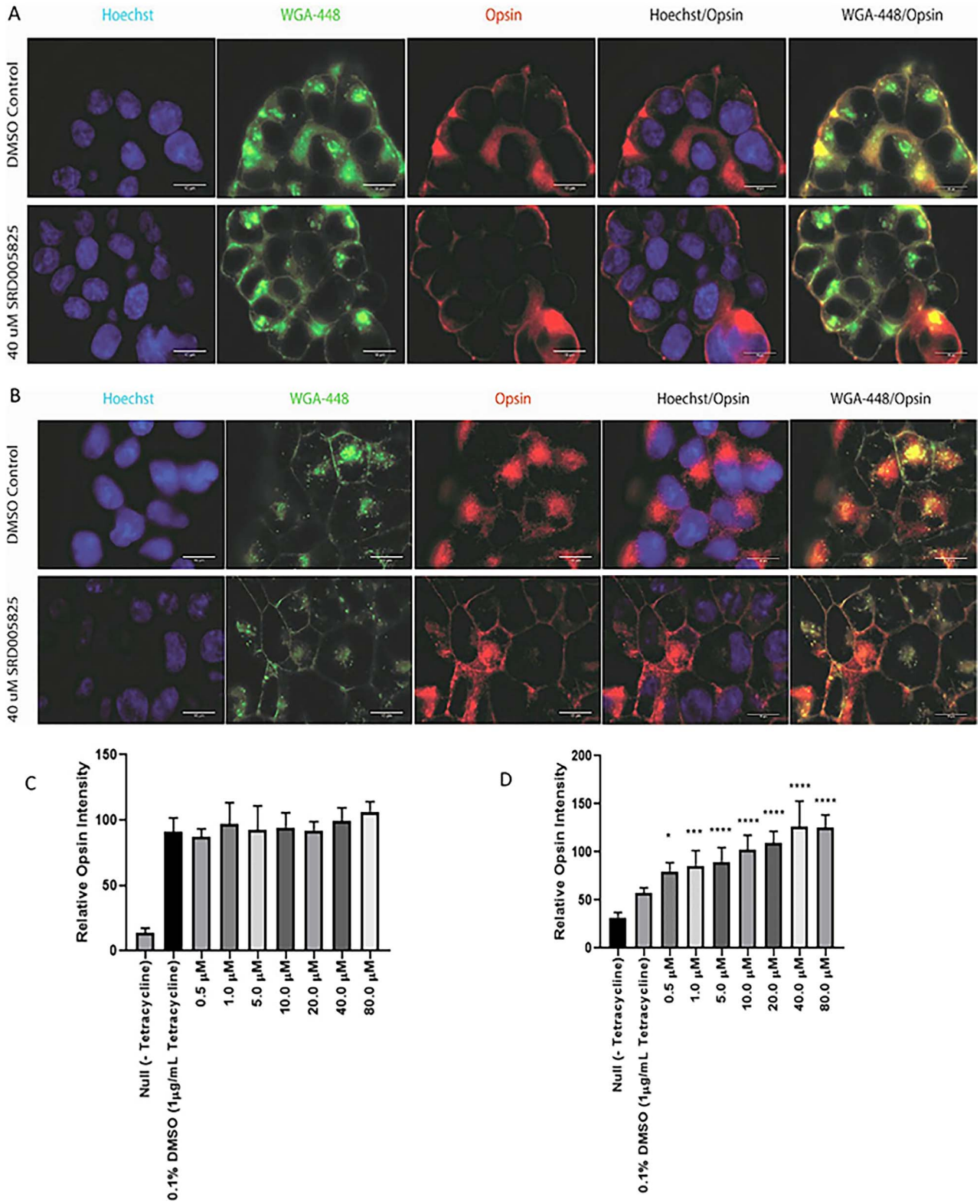

Figure 3. Membrane association of T17M rhodopsin facilitated by SRD005825. T-Rex-293 cells were induced to express wild-type (A, C) or T17M opsin (B, D). (A) Confocal microscopy of wild-type opsin expressing cells by Hoechst stain for DNA, Alexa Fluor 488 labeled WGA for plasma membrane, and 1D4 antibody for opsin after treatment with either DMSO (*top*) or 40 µM SRD005825 (*bottom*). (B) Confocal microscopy of T17M opsin-expressing cells by Hoechst stain, WGA-488, and 1D4 antibody after treatment with either DMSO (*top*) or 40 µM

→

←
SRD005825 (*bottom*). (C) Fluorescence intensity of plasma membrane-associated wild-type opsin after treatment at increasing concentrations of SRD005825. (D) Fluorescence intensity of plasma membrane-associated T17M opsin after treatment at increasing concentrations of SRD005825. The wild-type and T17M opsin-expressing cell lines represent two separate cell lines and were, thus, analyzed separately. The fluorescence intensities of membrane-associated opsin after treatment with SRD005825 were compared to the DMSO treatment of the same type of opsin. Null signifies the level of background fluorescence level in the absence of tetracycline induction. The *error bars* indicate standard deviation, and the *P* value determined by 1-way ANOVA is listed for conditions that showed significant difference from the DMSO control. $N = 10$ replicates; *$P < 0.05$; ***$P < 0.001$; ****$P < 0.0001$.

Treatment of Mice With SRD005825

To determine if the chaperone activity of SRD005825 could slow down the degeneration seen in T17M *RHO* transgenic mice, we treated T17M *RHO* transgenic mice on the mouse *Rho*+/+ background (T17M *RHO*::*Rho*+/+) by daily oral gavage. By 1 month of age, the ERG a-wave amplitude of T17M *RHO*::*Rho*+/+ is less than 50% that of wild-type littermates, and the amplitude decreased by an additional 50% by 3 months of age (data not shown). Therefore, we began treatment on postnatal day 14 and concluded treatment by 2 months of age. Retinal degeneration was monitored by SD-OCT analysis at 3, 5, and 7 weeks of age. T17M mice are extremely sensitive to white light illumination[19] so that ERG analysis was performed only once, on the last day before euthanasia of the mice for enucleation. Preliminary pharmacokinetic studies revealed that female mice required twice the oral dose of SRD005825 to achieve the same level of drug in the plasma and retina (Table 2). Consequently, the dose for male mice was 120 mg/kg and that for female mice was 240 mg/kg. Over the course of the experiments, we observed no adverse effects of the drug, and mice gained weight at the same rate as controls treated only with vehicle.

Protection of Retinal Structure by Treatment With SRD005825

The thickness of the ONL as determined by SD-OCT in live mice and by morphometry in formalin-fixed tissue was taken as a measure of retinal integrity. Progression ONL thinning was significant over the course of the study. Thus, there was an adequate assay window to determine efficacy in this model (~50% ONL thinning over the 7-week treatment duration). By 3 weeks of treatment, the difference in retinal thickness between drug-treated and control mice was evident (Figs. 5A, 5B). Both male and female mice dosed with SRD005825 showed increased ONL thickness compared with the vehicle-treated mice over the treatment course, and the impact of treatment was approximately the same in males and females. Although the retinas of treated mice thinned by two-thirds over the course of the experiment, the ONL of treated eyes remained twice as thick as the ONL of vehicle-treated T17M *RHO* mice (Figs. 5C, 5D). The benefit to retinal structure was also evident by morphometric measurement of the posterior retina following the 7-week dosing regimen (Fig. 6). Representative low-magnification images of the posterior retinas of wild-type, drug-treated, and vehicle-treated mice are shown in Figures 6A–6C. In mice treated with SRD005825, the ONL thickness was nearly 50% greater than vehicle-treated animals ($P = 0.03$).

Relative Improvement in Light Response Following Treatment With SRD005825

Because T17M mice are sensitive to illumination, ERG was performed only once (White A, et al. *IOVS*. 2006;47:ARVO E-Abstract 1059) at the conclusion of the dosing regimen (Fig. 7). We carried out 2-way ANOVA followed by Sidak multiple comparison test to identify statistically significant differences at each intensity. The corresponding *P* values are indicated in Figure 7B. There was preservation of scotopic a-wave and b-wave amplitudes in mice that were treated with SRD005825 compared with the vehicle-treated mice, although the difference in a-wave amplitudes was statistically significant only at the highest flash intensity that elicits a combine rod and cone response. Thus, the preservation of retinal structure observed by SD-OCT corresponded to a protection of retinal function as a consequence of treatment of T17M mice. The ERG response is in accord with the retinal thickness measurements by SD-OCT, which indicates preservation of approximately 30% of the retinal thickness following the 7-week time course.

Discussion

Because rhodopsin is so abundant in rod photoreceptors, misfolding of this protein can easily

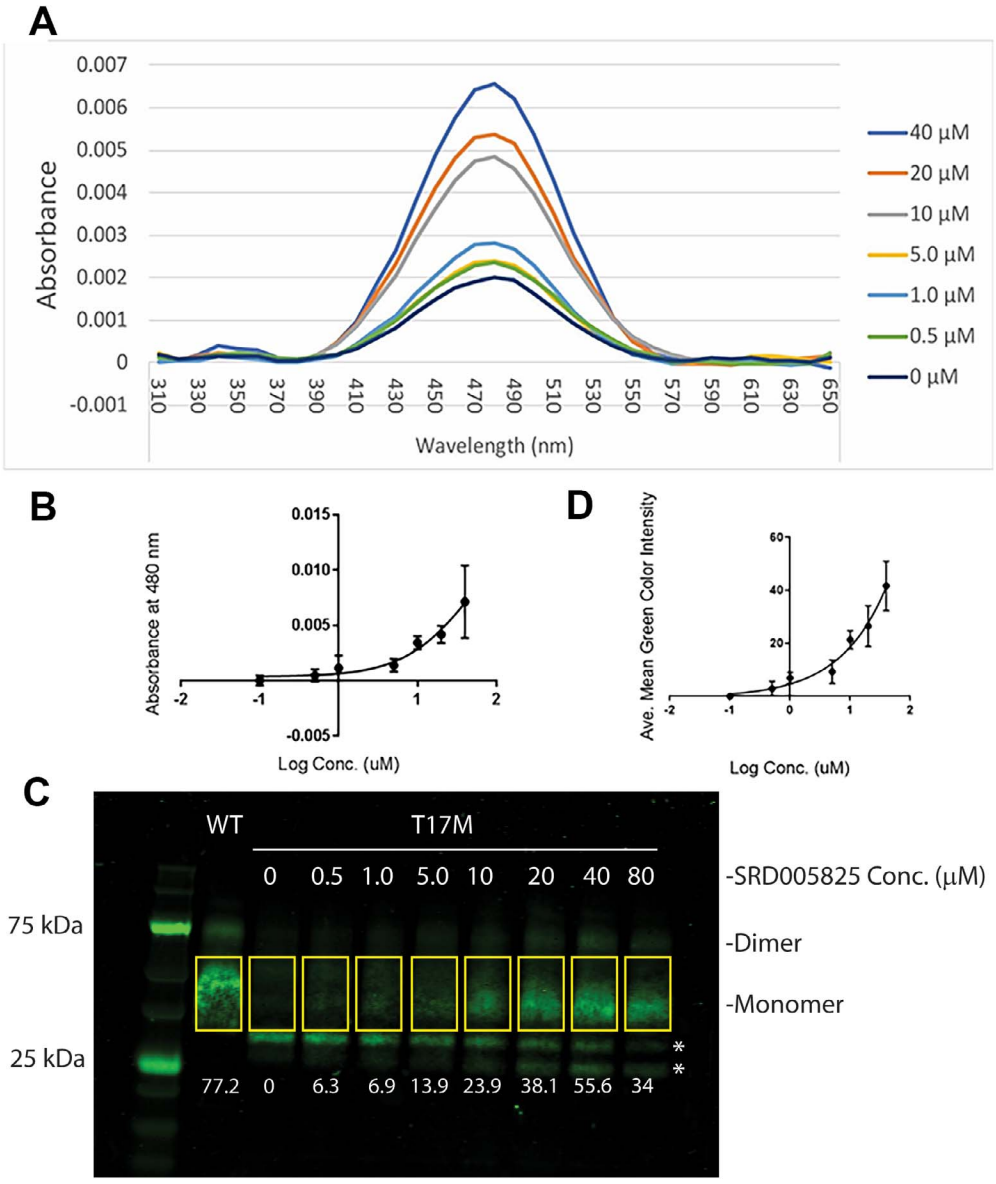

Figure 4. Generation of functional T17M rhodopsin after treatment with SRD005825. T-Rex-293 cells expressing human T17M opsin were induced for expression and incubated at increasing concentrations of SRD005825. (A) Absorbance spectrum of immunoaffinity-purified T17M rhodopsin from SRD005825-treated T17M-expressing cells, and the rhodopsin peak at 480 nm at increasing concentrations of SRD005825. (B) The plot of OD 480 nm from A as a function of concentration of SRD005825. (C) Western blot using 1D4 antibody of the same T17M rhodopsin samples as in 4 and the comparison to wild-type rhodopsin produced in T-Rex-293 cells. The relative quantities of monomeric T17M opsin were estimated by mean intensity of each band, from three replicates of the experiment (Supplementary Table S1). Numbers at the *bottom* of each lane represent the mean *green* color intensity of monomeric T17M opsin within *rectangles* (using Photoshop CC). *Asterisks* indicate presumptive proteolytic fragments or nonglycosylated forms of opsin that react with the C-terminal-specific antibody. (D) The plot of relative quantity of T17M rhodopsin as a function of concentration of SRD005825. Due to the toxic effects of SRD005825 at or above 80 µM to the cells, no EC_{50} could be determined.

overcome the capacity of ER-associated degradation and proteasomal degradation,[41,42] leading to prolonged induction of the unfolded protein response and eventually to cell death.[23,43,44] In transgenic mice expressing T17M opsin, the human rhodopsin induces ER stress.[20] These mice are extremely sensitive to light damage,[19] perhaps because some of the opsin reconstitutes with 11-cis-retinal and traverses to the outer segments.[16]

Given that photoreceptor death in class II mutations of *RHO* is associated with protein misfolding, the delivery of chaperone proteins or small molecules is an

Table 2. Pharmacokinetic Parameters of SRD005825

Dose Level (mg/kg)	Sex	C_{max} Plasma (ng/g)	C_{max} Plasma (nmole/g)	C_{max} Retina (ng/g)	C_{max} Retina (nmole/g)	$t_{1/2}$ Retina (hour)
20	Male	1380	4.69	1410	4.79	0.854
20	Female	427	1.45	627	2.13	0.556
40	Male	5760	19.58	6970	23.70	1.12
40	Female	2740	9.32	2670	9.08	1.21
120	Male	27700	94.18	27700	94.18	4.24
120	Female	12500	42.50	8820	29.99	1.09

C_{max}, maximum concentration in plasma or retina after a single dose; $t_{1/2}$, observed elimination half-life.

attractive approach for protecting the retina, especially in slowly progressing patients.[25] SRD005825 was designed precisely for this purpose. SRD005825 was well tolerated by the mice in our study, and in separate studies it was well tolerated in rats and dogs as well (data not shown). In cells, SRD005825 led to the increased association of T17M opsin with the plasma membrane and decreased accumulation of the protein in the ER (Fig. 3B). As intended, the compound exhibited a dose-dependent capability to permit reconstitution of T17M rhodopsin (Fig. 4). These are the hallmarks of an effective pharmacologic chaperone.

It should be noted that increased transport of mutant rhodopsin may not be beneficial for all adRP mutations in *RHO*. For example, Athanasiou et al.[45] reported that metformin increased transport of P23H rhodopsin to outer segments of P23H knock-in mice but led to increased retinal degeneration in P23H *Rho* transgenic rats. In contrast, Moritz and Tam[46] demonstrated that 11-cis retinal acts as a chaperone for the proper folding and transport of P23H rhodopsin, facilitating its exit from the ER. They suggested that the light sensitivity of P23H transgenic *Xenopus leavis* retinas is associated with the light-induced destruction of the chromophore. Therefore, in this organism under these environmental conditions, improved transport of P23H rhodopsin is protective. It is likely that the benefit of SRD005825 as a pharmacologic chaperone will depend on the mutation and on the preclinical model and environmental conditions used to test it, and care must be taken to select the appropriate human patients for a clinical trial.

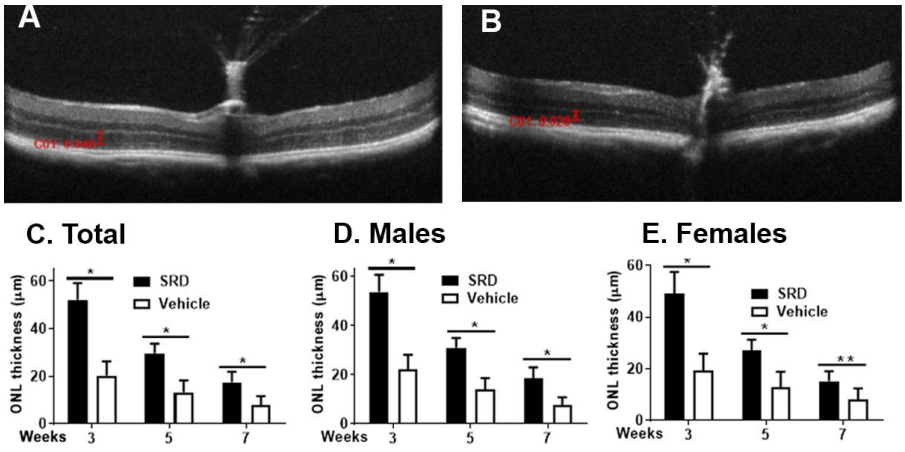

Figure 5. Oral treatment with SRD005825 reduces the rate of ONL thinning in T17M *RHO* transgenic mice. Mice were treated by daily gavage with 120 mg/kg (males) or 240 mg/kg (females) beginning on postnatal day 14. The thickness of the ONL was measured by SD-OCT at 3, 5, and 7 weeks following the beginning of drug delivery. Control mice were treated with the vehicle. Measurements were made at four positions equidistant to the optic nerve head and averaged for each eye. (A) Representative OCT b-scan from mouse treated with SRD005925 at the 3-week time point. (B) Image from a vehicle-treated mouse at the same time point. (C–E) Average ONL thickness from SRD005825- and vehicle-treated mice at 3, 5, and 7 weeks. (C) Total mice, (D) males, and (E) females. The *error bars* indicate standard deviation. SRD005825-treated males, $N = 14$; SRD005825-treated females, $N = 7$; vehicle-treated males, $N = 5$; vehicle-treated females, $N = 7$. *$P < 0.05$; **$P < 0.01$.

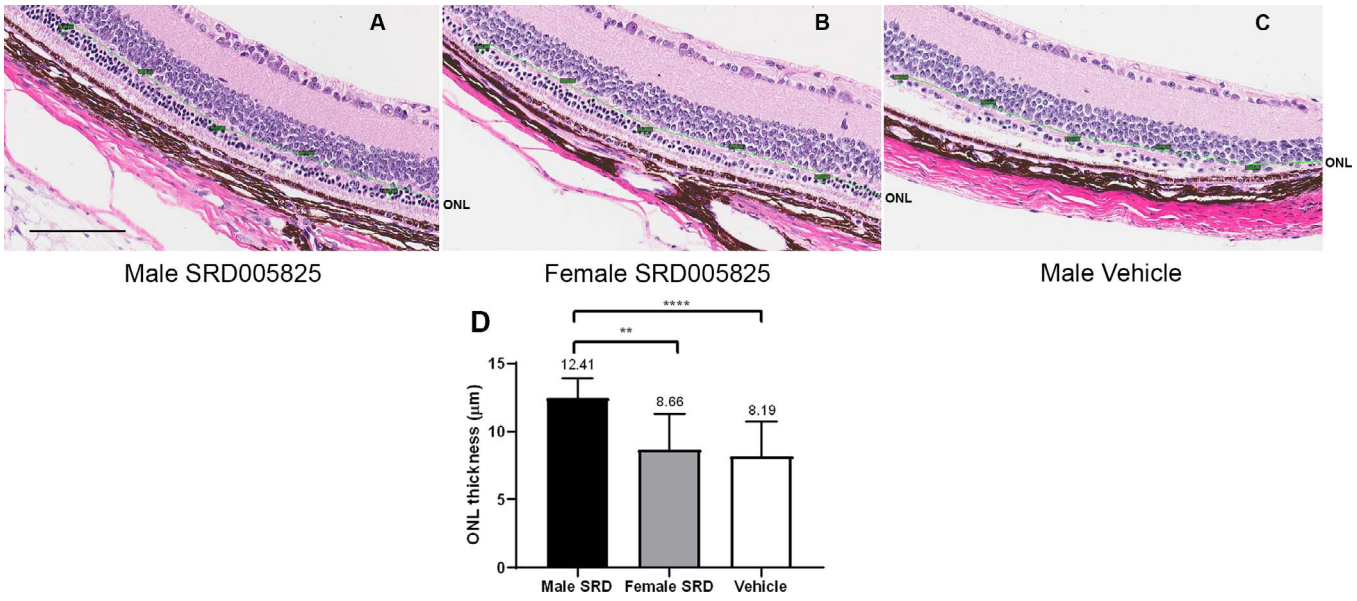

Figure 6. Treatment with SRD005825 partially protects the outer retina in T17M *RHO* mice. Following 7 weeks of treatment, mice were humanely euthanized, and eyes were fixed in 4% paraformaldehyde and prepared for paraffin embedding, sectioning, and staining with hematoxylin and eosin. *Scale bars* are 100 microns. Quantification was made by measuring the ONL thickness at three positions at either side of the optic nerve head. The six measurements were averaged for each eye, and the two eyes were averaged for each mouse. (A) Example male SRD005825-treated T17M mouse retina; (B) example of female SRD005825-treated T17M *RHO* mouse retina; (C) male T17M *RHO* vehicle-treated retina. (D) Quantification of ONL thickness. (Male SRD = 17; Female SRD = 6; Vehicle = 9). *Error bars* represent standard deviations. $^{**}P < 0.01$; $^{****}P < 0.0001$.

The half-lives of SRD005825 in the retina at all dose levels were short (Table 2). At the 120-mg/kg dose level, the half-life values were 4.24 and 1.09 hours for male and female mice, respectively. For all dose groups, the area under the curve (AUC) of the compound in the retina was comparable to that of the plasma. The AUC ratios retina:plasma were between 0.844 and 1.37 (data not shown). SRD005825 is not able to compete with 11-cis-retinal (or 9-cis-retinal) once the endogenous ligand is bound, suggesting that SRD005825 binds to T17M opsin in the ER, in the absence of 11-cis-retinal, to chaperone opsin to the membrane surface. In cell culture, micromolar levels of SRD005825 facilitated membrane translocation of opsin. Assuming that the density of retinal tissue is 1 gm/ml[47], the concentration of drug in the retina at the high dose reached 94 µM for males and 30 µM for females, well within the range needed to facilitate transport of opsin. Although treatment with SRD005825 did not prevent retinal degeneration in T17M *RHO* transgenic mice, it significantly delayed the loss of photoreceptor cells. Following 3 weeks of treatment, the ONL thickness (55.0 µm) was only slightly less than wild-type mice of the same age (64.5 µm) At every measurement, drug-treated mice retained twice the thickness of the ONL compared with the vehicle-treated mice. Relative protection was confirmed by histology at the conclusion of the experiment (Fig. 6). We note that protection of ONL thickness as measured by histology was not significant for female mice, although significant protection of this structure in females was demonstrated by OCT. We attribute this difference to sampling error because only a subset of mice were used for morphometry.

ERG measurements (Fig. 7) also indicated a protection of retinal function. Unfortunately, we could assess the ERG response only at the conclusion of the experiment because of the extreme sensitivity of T17M transgenic mice to light injury (White A, et al. *IOVS.* 2006;47:ARVO E-Abstract 1059), and therefore, we could not measure an impact of treatment on the rate of retinal degeneration by using this method. Nevertheless, at the final time point, it was clear that the ERG b-wave was relatively preserved in SRD005825-treated mice, indicating enhanced protection of the inner retina, or improved response of the bipolar cells, to the signals generated by remaining rods. It appeared that females might show better protection of the photoreceptor response (ERG a-wave) in response to treatment than males, but this may be because the vehicle-treated females exhibited comparatively lower

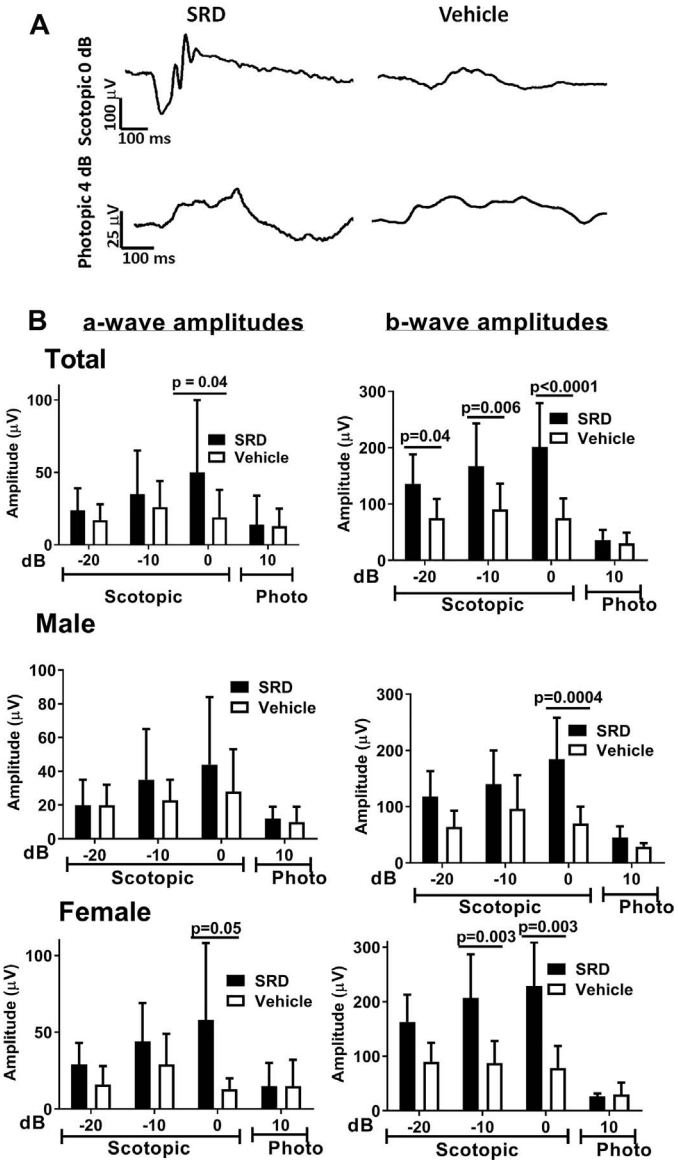

Figure 7. Preservation of retinal function by treatment with SRD005825. ERG was performed on dark-adapted, anesthetized T17M transgenic mice following 7 weeks of treatment with SRD005925 or vehicle, using an LKC Electrodiagnostic System to deliver flashes at –20 dB (0.025 cd·sec/m^2), –10 dB (0.25 cd·sec/m^2), and 0 dB (2.5 cd·sec/m^2). Following 2 minutes of photobleaching, with constant white light, photopic ERG responses were recorded, and the response to 10-dB flashes is reported. (A) Representative wave forms of scotopic (at 0 dB) and photopic (10 dB) electroretinograms from SRD005825-treated and vehicle-treated mice. Male a, $N = 12$; SRD005825-treated females, $N = 8$; vehicle-treated males, $N = 4$; vehicle-treated females, $N = 6$. *Error bars* indicate standard deviations. *P* values indicated in the figure were determined by 2-way ANOVA using the Sidak method for multiple comparisons.

a-wave amplitudes than vehicle-treated males. There was no impact of treatment on the photopic ERG amplitudes.

Although we have demonstrated that SRD005825 acts as pharmacologic chaperone in cells and that it delays retinal degeneration in mice, we have not demonstrated that it improves the folding or the trafficking of T17M rhodopsin in vivo. Given its rapid elimination from the retina (Table 2) and its lower affinity for opsin than 11-cis-retinal, it may not be present at a high enough concentration to affect rhodopsin folding hours after dosing. Because the prevention of retinal binding prevented retinal degeneration in T17M transgenic frogs,[15] SRD005825 may reduce toxicity by reducing the reconstitution of rhodopsin (Fig. 2). An alternative explanation is that SRD005825 somehow affects the levels of retinoids in the eye and, thereby, reduces the toxicity of T17M rhodopsin. Determining the actual mechanism of protection will require additional experimentation.

The T17M mutation in rhodopsin falls into the clinical class B mutations because patients retain normal rods into adulthood and the disease frequently spares the superior retina.[48] This makes patients with T17M *RHO* excellent candidates for development of therapy. In their exhaustive and incisive molecular simulation and virtual screening experiments, Behnen and colleagues[28] identified another retinal analogue that exhibited chaperone-like activities in cells. Like SRD005825, this compound also appeared to compete with 9-cis-retinal for binding to opsin. It was noteworthy that this compound (13-cis-5,8-ERA) was more effective in promoting the folding and transport of the P23H and E181K mutations than it was for the T17M mutation. Therefore, as noted above, it is likely that SRD005825 will show differential effects on different *RHO* mutations.

Although gene therapy is being developed for the treatment of adRP[49-53] not all patients will be good candidates for that approach, and some who will possibly benefit from gene therapy may have to wait for the availability of treatment. In addition, disorganization of the inner retina is likely to occur as the outer retina degenerates.[13] For these reasons, developing drugs that prolong the survival of rod photoreceptors remains an important area of research for the prevention of blindness due to adRP. Should SRD005825 prove safe in people and retard retinal degeneration caused by a spectrum of *RHO* mutations, it should be considered as a candidate for therapy.

Acknowledgments

The authors thank Sophia Park for assistance with the PNGase F experiment and Hong Li for assistance with OCT analysis. The study was funded by Shire HGT Inc., Lexington, MA, a Takeda Company. Additional support came from the Shaler Richardson Professorship endowment to ASL.

The rights to the compound reported in this paper are licensed by Shire HGT, a Takeda company.

Author contributions were as follows: Chulbul M. Ahmed, in vivo study in treatment of T17M mice with small-molecule chaperone; Brian T. Dwyer, in vitro assay for rhodopsin generation and T17M translocation, data analysis; Alla Romashko, in vitro assay for competition of wild-type rhodopsin by small-molecule chaperone; Eun-Hee Park, generation of human Rho cell line; Steve Van Adestine (Covance), measurement of thickness of the ONL; Zhen Lou, in vivo pharmacokinetic/pharmacodynamic (PK/PD) study in T17M mice; Devin Welty, in vivo PK/PD study in T17M mice; Serene Josiah, project leader, in vivo and in vitro study design, and data analysis; Anneli Savinainen, in vivo study design and execution, data analysis; Bohong Zhang, in vitro study design and execution, data analysis; and Alfred S. Lewin, characterization of T17M RHO mouse model and in vivo efficacy study design and data analysis.

Disclosure: **C.M. Ahmed**, None; **B.T. Dwyer**, Shire HGT, a Takeda Company (E); **A. Romashko**, Shire HGT, a Takeda Company (E); **S. Van Adestine**, None; **E.-H. Park**, Shire HGT, a Takeda Company (E); **Z. Lou**, Shire HGT, a Takeda Company (E); **D. Welty**, Shire HGT, a Takeda Company (E); **S. Josiah**, Shire HGT, a Takeda Company (E); **A. Savinainen**, Shire HGT, a Takeda Company (E); **B. Zhang**, Shire HGT, a Takeda Company (E); **A.S. Lewin**, Shire HGT, a Takeda Company (F)

References

1. Daiger SP, Sullivan LS, Bowne SJ. Genes and mutations causing retinitis pigmentosa. *Clin Genet*. 2013;84;132–141.
2. Laboratory for the Molecular Diagnosis of Inherited Eye Diseases. RetNet Retinal Information Network. https://sph.uth.edu/retnet/home.htm. Accessed June 23, 2019.
3. Sullivan LS, Bowne SJ, Birch DG, et al. Prevalence of disease-causing mutations in families with autosomal dominant retinitis pigmentosa: a screen of known genes in 200 families. *Invest Ophthalmol Vis Sci*. 2006;47:3052–3064.
4. Liang Y, Fotiadis D, Filipek S, Saperstein DA, Palczewski K, Engel A. Organization of the G protein-coupled receptors rhodopsin and opsin in native membranes. *J Biol Chem*. 2003;278:21655–21662.
5. Athanasiou D, Aguila M, Bellingham J, et al. The molecular and cellular basis of rhodopsin retinitis pigmentosa reveals potential strategies for therapy. *Prog Retin Eye Res*. 2018;62:1–23.
6. Mendes HF, van der Spuy J, Chapple JP, Cheetham ME. Mechanisms of cell death in rhodopsin retinitis pigmentosa: implications for therapy. *Trends Mol Med*. 2005;11:177–185.
7. Gorbatyuk MS, Knox T, LaVail MM, et al. Restoration of visual function in P23H rhodopsin transgenic rats by gene delivery of BiP/Grp78. *Proc Natl Acad Sci U S A*. 2010;107:5961–5966.
8. Athanasiou D, Aguila M, Bellingham J, Kanuga N, Adamson P, Cheetham ME. The role of the ER stress-response protein PERK in rhodopsin retinitis pigmentosa. *Hum Mol Genet*. 2017;26:4896–4905.
9. Shinde VM, Sizova OS, Lin JH, LaVail MM, Gorbatyuk MS. ER stress in retinal degeneration in S334ter Rho rats. *PLoS One*. 2012;7:e33266.
10. Chiang WC, Kroeger H, Sakami S, et al. Robust endoplasmic reticulum-associated degradation of rhodopsin precedes retinal degeneration. *Mol Neurobiol*. 2015;52:679–695.
11. Campochiaro PA, Mir TA. The mechanism of cone cell death in Retinitis Pigmentosa. *Prog Retin Eye Res*. 2018;62:24–37.
12. Ait-Ali N, Fridlich R, Millet-Puel G, et al. Rod-derived cone viability factor promotes cone survival by stimulating aerobic glycolysis. *Cell*. 2015;161:817–832.
13. Jones BW, Pfeiffer RL, Ferrell WD, Watt CB, Marmor M, Marc RE. Retinal remodeling in human retinitis pigmentosa. *Exp Eye Res*. 2016;150:149–165.
14. Li ZY, Jacobson SG, Milam AH. Autosomal dominant retinitis pigmentosa caused by the threonine-17-methionine rhodopsin mutation: retinal histopathology and immunocytochemistry. *Exp Eye Res*. 1994;58:397–408.
15. Tam BM, Moritz OL. The role of rhodopsin glycosylation in protein folding, trafficking, and

light-sensitive retinal degeneration. *J Neurosci*. 2009;29:15145–15154.
16. Tam BM, Noorwez SM, Kaushal S, Kono M, Moritz OL. Photoactivation-induced instability of rhodopsin mutants T4K and T17M in rod outer segments underlies retinal degeneration in *X. laevis* transgenic models of retinitis pigmentosa. *J Neurosci*. 2014;34:13336–13348.
17. Li T, Sandberg MA, Pawlyk BS, et al. Effect of vitamin A supplementation on rhodopsin mutants threonine-17 – > methionine and proline-347 –> serine in transgenic mice and in cell cultures. *Proc Natl Acad Sci U S A*. 1998;95:11933–11938.
18. Krebs MP, White DA, Kaushal S. Biphasic photoreceptor degeneration induced by light in a T17M rhodopsin mouse model of cone bystander damage. *Invest Ophthalmol Vis Sci*. 2009;50:2956–2965.
19. White DA, Fritz JJ, Hauswirth WW, Kaushal S, Lewin AS. Increased sensitivity to light-induced damage in a mouse model of autosomal dominant retinal disease. *Invest Ophthalmol Vis Sci*. 2007;48:1942–1951.
20. Kunte MM, Choudhury S, Manheim JF, et al. ER stress is involved in T17M rhodopsin-induced retinal degeneration. *Invest Ophthalmol Vis Sci*. 2012;53:3792–3800.
21. Murray AR, Vuong L, Brobst D, et al. Glycosylation of rhodopsin is necessary for its stability and incorporation into photoreceptor outer segment discs. *Hum Mol Genet*. 2015;24:2709–2723.
22. Choudhury S, Bhootada Y, Gorbatyuk O, Gorbatyuk M. Caspase-7 ablation modulates UPR, reprograms TRAF2-JNK apoptosis and protects T17M rhodopsin mice from severe retinal degeneration. *Cell Death Dis*. 2013;4:e528.
23. Jiang H, Xiong S, Xia X. Retinitis pigmentosa associated rhodopsin mutant T17M induces endoplasmic reticulum (ER) stress and sensitizes cells to ER stress-induced cell death. *Mol Med Rep*. 2014;9:1737–1742.
24. Chiang WC, Hiramatsu N, Messah C, Kroeger H, Lin JH. Selective activation of ATF6 and PERK endoplasmic reticulum stress signaling pathways prevent mutant rhodopsin accumulation. *Invest Ophthalmol Vis Sci*. 2012;53:7159–7166.
25. Mendes HF, Cheetham ME. Pharmacological manipulation of gain-of-function and dominant-negative mechanisms in rhodopsin retinitis pigmentosa. *Hum Mol Genet*. 2008;17:3043–3054.
26. Tao YX, Conn PM. Pharmacoperones as novel therapeutics for diverse protein conformational diseases. *Physiol Rev*. 2018;98:697–725.
27. Noorwez SM, Malhotra R, McDowell JH, Smith KA, Krebs MP, Kaushal S. Retinoids assist the cellular folding of the autosomal dominant retinitis pigmentosa opsin mutant P23H. *J Biol Chem*. 2004;279:16278–16284.
28. Behnen P, Felline A, Comitato A, et al. A small chaperone improves folding and routing of rhodopsin mutants linked to inherited blindness. *iScience* 2018;4:1–19.
29. Palczewski K. Retinoids for treatment of retinal diseases. *Trends Pharmacol Sci*. 2010;31:284–295.
30. Lou Z, Braga T, Welty D, et al. Metabolism of 14C-SRD005825 in mouse, rat, dog, monkey, and human hepatic microsomes. *Drug Metab Pharmacokinet*. 2018;33:S81.
31. Luo G, Welty D, Leitz S, et al. Identification of human cyp enzymes involved in the metabolism of 14C-SRD005825. *Drug Metab Pharmacokinet*. 2018;33:S80–S81.
32. Noorwez SM, Ostrov DA, McDowell JH, Krebs MP, Kaushal S. A high-throughput screening method for small-molecule pharmacologic chaperones of misfolded rhodopsin. *Invest Ophthalmol Vis Sci*. 2008;49:3224–3230.
33. Chen Y, Chen Y, Jastrzebska B, et al. A novel small molecule chaperone of rod opsin and its potential therapy for retinal degeneration. *Nat Commun*. 2018;9:1976.
34. Noorwez SM, Kuksa V, Imanishi Y, et al. Pharmacological chaperone-mediated in vivo folding and stabilization of the P23H-opsin mutant associated with autosomal dominant retinitis pigmentosa. *J Biol Chem*. 2003;278:14442–14450.
35. Noorwez SM, Sama RR, Kaushal S. Calnexin improves the folding efficiency of mutant rhodopsin in the presence of pharmacological chaperone 11-cis-retinal. *J Biol Chem*. 2009;284:33333–33342.
36. Krebs MP, Holden DC, Joshi P, Clark CL III, Lee AH, Kaushal S. Molecular mechanisms of rhodopsin retinitis pigmentosa and the efficacy of pharmacological rescue. *J Mol Biol*. 2010;395:1063–1078.
37. Chang B, Hurd R, Wang J, Nishina P. Survey of common eye diseases in laboratory mouse strains. *Invest Ophthalmol Vis Sci*. 2013;54:4974–4981.
38. Biswal MR, Ahmed CM, Ildefonso CJ, et al. Systemic treatment with a 5HT1a agonist induces anti-oxidant protection and preserves the retina

from mitochondrial oxidative stress. *Exp Eye Res*. 2015;140:94–105.
39. Opefi CA, South K, Reynolds CA, Smith SO, Reeves PJ. Retinitis pigmentosa mutants provide insight into the role of the N-terminal cap in rhodopsin folding, structure, and function. *J Biol Chem*. 2013;288:33912–33926.
40. Hodges RS, Heaton RJ, Parker JM, Molday L, Molday RS. Antigen-antibody interaction. Synthetic peptides define linear antigenic determinants recognized by monoclonal antibodies directed to the cytoplasmic carboxyl terminus of rhodopsin. *J Biol Chem*. 1988;263:11768–11775.
41. Illing ME, Rajan RS, Bence NF, Kopito RR. A rhodopsin mutant linked to autosomal dominant retinitis pigmentosa is prone to aggregate and interacts with the ubiquitin proteasome system. *J Biol Chem*. 2002;277:34150–34160.
42. Lobanova ES, Finkelstein S, Li J, et al. Increased proteasomal activity supports photoreceptor survival in inherited retinal degeneration. *Nat Commun*. 2018;9:1738–1738.
43. Gorbatyuk MS, Knox T, LaVail MM, et al. Restoration of visual function in P23H rhodopsin transgenic rats by gene delivery of BiP/Grp78. *Proc Natl Acad Sci U S A*. 2010;107:5961–5966.
44. Lin JH, Li H, Yasumura D, et al. IRE1 Signaling affects cell fate during the unfolded protein response. *Science*. 2007;318:944–949.
45. Athanasiou D, Aguila M, Opefi CA, et al. Rescue of mutant rhodopsin traffic by metformin-induced AMPK activation accelerates photoreceptor degeneration. *Hum Mol Genet*. 2017;26:305–319.
46. Moritz OL, Tam BM. Recent insights into the mechanisms underlying light-dependent retinal degeneration from X. laevis models of retinitis pigmentosa. *Adv Exp Med Biol*. 2010;664:509–515.
47. IT'IS Foundation. Tissue properties. https://itis.swiss/virtual-population/tissue-properties/database/density/. Accessed July 17, 2019.
48. Cideciyan AV, Hood DC, Huang Y, et al. Disease sequence from mutant rhodopsin allele to rod and cone photoreceptor degeneration in man. *Proc Natl Acad Sci U S A*. 1998;95:7103–7108.
49. Millington-Ward S, Chadderton N, O'Reilly M, et al. Suppression and replacement gene therapy for autosomal dominant disease in a murine model of dominant retinitis pigmentosa. *Mol Ther*. 2011;19:642–649.
50. Cideciyan AV, Sudharsan R, Dufour VL, et al. Mutation-independent rhodopsin gene therapy by knockdown and replacement with a single AAV vector. *Proc Natl Acad Sci U S A*. 2018;115:E8547–E8556.
51. Tsai YT, Wu WH, Lee TT, et al. Clustered regularly interspaced short palindromic repeats-based genome surgery for the treatment of autosomal dominant retinitis pigmentosa. *Ophthalmology*. 2018;125:1421–1430.
52. Mussolino C, Sanges D, Marrocco E, et al. Zinc-finger-based transcriptional repression of rhodopsin in a model of dominant retinitis pigmentosa. *EMBO Mol Med*. 2011;3:118–128.
53. Greenwald DL, Cashman SM, Kumar-Singh R. Mutation-independent rescue of a novel mouse model of retinitis pigmentosa. *Gene Ther*. 2013;20:425–434.